



LJMU Research Online

Lund, M, Heaton, R, Hargreaves, IP, Gregersen, N and Olsen, RKJ

Odd- and even-numbered medium-chained fatty acids protect against glutathione depletion in very long-chain acyl-CoA dehydrogenase deficiency

<https://researchonline.ljmu.ac.uk/id/eprint/18107/>

Article

Citation (please note it is advisable to refer to the publisher's version if you intend to cite from this work)

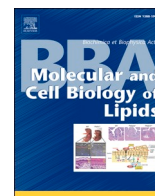
**Lund, M, Heaton, R, Hargreaves, IP ORCID logoORCID:
<https://orcid.org/0000-0002-2760-5603>, Gregersen, N and Olsen, RKJ (2022)
Odd- and even-numbered medium-chained fatty acids protect against
glutathione depletion in very long-chain acyl-CoA dehydrogenase**

LJMU has developed [LJMU Research Online](#) for users to access the research output of the University more effectively. Copyright © and Moral Rights for the papers on this site are retained by the individual authors and/or other copyright owners. Users may download and/or print one copy of any article(s) in LJMU Research Online to facilitate their private study or for non-commercial research. You may not engage in further distribution of the material or use it for any profit-making activities or any commercial gain.

The version presented here may differ from the published version or from the version of the record. Please see the repository URL above for details on accessing the published version and note that access may require a subscription.

For more information please contact researchonline@ljmu.ac.uk

<http://researchonline.ljmu.ac.uk/>



Odd- and even-numbered medium-chained fatty acids protect against glutathione depletion in very long-chain acyl-CoA dehydrogenase deficiency

Martin Lund^{a,*}, Robert Heaton^b, Iain P. Hargreaves^b, Niels Gregersen^a, Rikke K.J. Olsen^{a,*}

^a Research Unit for Molecular Medicine, Department of Clinical Medicine, Aarhus University and Aarhus University Hospital, Palle Juul-Jensens Boulevard 99, 8200 Aarhus, Denmark

^b School of Pharmacy, Liverpool John Moore University, Byrom Street, Liverpool L3 3AF, United Kingdom

ARTICLE INFO

Keywords:

Mitochondria
Glutathione
Anaplerosis
Heptanoate
Octanoate
Oxidative stress
VLCAD
Fatty acids oxidation deficiency

ABSTRACT

Recent trials have reported the ability of triheptanoin to improve clinical outcomes for the severe symptoms associated with long-chain fatty acid oxidation disorders, including very long-chain acyl-CoA dehydrogenase (VLCAD) deficiency.

However, the milder myopathic symptoms are still challenging to treat satisfactorily. Myopathic pathogenesis is multifactorial, but oxidative stress is an important component. We have previously shown that metabolic stress increases the oxidative burden in VLCAD-deficient cell lines and can deplete the antioxidant glutathione (GSH).

We investigated whether medium-chain fatty acids provide protection against GSH depletion during metabolic stress in VLCAD-deficient fibroblasts. To investigate the effect of differences in anaplerotic capacity, we included both even-(octanoate) and odd-numbered (heptanoate) medium-chain fatty acids. Overall, we show that modulation of the concentration of medium-chain fatty acids in culture media affects levels of GSH retained during metabolic stress in VLCAD-deficient cell lines but not in controls.

Lowered glutamine concentration in the culture media during metabolic stress led to GSH depletion and decreased viability in VLCAD deficient cells, which could be rescued by both heptanoate and octanoate in a dose-dependent manner. Unlike GSH levels, the levels of total thiols increased after metabolic stress exposure, the size of this increase was not affected by differences in cell culture medium concentrations of glutamine, heptanoate or octanoate.

Addition of a PPAR agonist further exacerbated stress-related GSH-depletion and viability loss, requiring higher concentrations of fatty acids to restore GSH levels and cell viability.

Both odd- and even-numbered medium-chain fatty acids efficiently protect VLCADdeficient cells against metabolic stress-induced antioxidant depletion.

1. Introduction

Very long-chain acyl-CoA dehydrogenase (VLCAD) deficiency was first described in 1993 and is currently a relatively well-understood disorder, and is part of newborn screening programmes in many countries [1–3]. The enzymatic function of VLCAD is to catalyse the initial dehydrogenation step of long-chain fatty acid esters during mitochondrial fatty acid oxidation (FAO). VLCAD can efficiently process fatty acids with chain lengths from 12 to 22 carbons [4].

Severe and moderate forms of VLCAD deficiency involve cardiac or hepatic phenotypes, with episodes of hypoketotic hypoglycaemia and

risk of sudden death. A third and comparatively mild phenotype is myopathic, presenting with cramps, pain, fatigue, weakness, and rhabdomyolysis [2,5]. Currently, therapy is based on lifestyle intervention, especially avoidance of fasting, fat-reduced diets and supplementation with medium-chain triglyceride (MCT). Medium-chain fatty acids are used as a standard therapeutic approach in the various long-chain FAO disorders, because of their ability to bypass the dysfunctional cellular machinery associated with the various inborn long-chain FAO disorders [2,6].

The main cellular factor causing symptoms is the failure to oxidise sufficient long-chain fatty acids in the mitochondria for maintenance of

* Corresponding authors at: Research Unit for Molecular Medicine, Aarhus University Hospital, Palle Juul-Jensens Boulevard 99, 8200 Aarhus, Denmark.

E-mail addresses: martin.lund@post.au.dk (M. Lund), rikke.olsen@clin.au.dk (R.K.J. Olsen).

<https://doi.org/10.1016/j.bbalip.2022.159248>

Received 11 January 2022; Received in revised form 9 October 2022; Accepted 17 October 2022

Available online 7 November 2022

1388-1981/© 2022 The Authors. Published by Elsevier B.V. This is an open access article under the CC BY license (<http://creativecommons.org/licenses/by/4.0/>).

energy homeostasis, measurable as decreased long-chain FAO flux [7,8]. Other contributors to the phenotype include accumulation of VLCAD substrates and related metabolites ("lipotoxicity"), sequestration of co-factors such as coenzyme A (CoA), cataplerotic stress and stress imposed by misfolded or absent VLCAD protein [2,6,7,9]. An important pathological aspect of VLCAD deficiency is the gradual development of the myopathic phenotype and secondary pathological traits, including secondary mitochondrial respiratory chain deficiency, reduced mitochondrial quality, increased production of reactive oxygen species (ROS), disruption of Ca²⁺ homeostasis and compromised amino acid metabolism [2,10–14].

However, the pathological driver(s) of these secondarily acquired dysfunctions are not well defined [5].

In a recent study, we found that treating VLCAD-deficient dermal fibroblasts with the PPAR agonist bezafibrate prior to metabolic stress exposure led to increased ROS production, depletion of the essential antioxidant tripeptide glutathione (GSH) and decreased cellular viability [15]. ROS is unusually deleterious in certain metabolic disorders, such as VLCAD deficiency, because of a reduced bioenergetic capacity for maintaining sufficient NADPH levels to power a fully functional antioxidant system. This has important consequences, such as oxidative stress mediated development of secondary metabolic deficiencies [5,12,14,16].

The mitochondrial antioxidant system is highly dependent on GSH and related enzymatic systems, all of which require NADPH to recycle oxidized GSH. NADPH production is dependent on the Krebs cycle and the inner membrane proton gradient in the mitochondrial matrix [17,18]. Mitochondrial FAO is a major electron contributor to the Krebs cycle, and the two pathways combined are the primary electron donors to the mitochondrial respiratory chain, which means that an intact FAO system is essential for maintaining matrix NADPH and GSH levels [12,17,18].

Apart from contributing electrons to the Krebs cycle, another primary function of FAO is to provide carbon for the Krebs cycle [19,20]. In VLCAD deficiency, the rate of carbon flux into the Krebs cycle can be reduced due to reduced FAO flux [7,9]. In both animal models and humans, VLCAD deficiency and other long-chain FAO disorders have been found to suffer from periodic cataplerotic stress [21–23]. This occurs despite a supply of acetyl-CoA from a high-carbohydrate and a low-fat diet supplemented with MCT.

Triheptanoin is a triglyceride containing three heptanoate fatty acids, a medium-chain fatty acid with a seven-carbon chain. Clinical trials of triheptanoin compared with MCT supplementation have shown a significant decrease in severe symptoms. However, a significant fraction of the milder myopathic events remained [22,24–27]. Heptanoate has an anaplerotic profile superior to even-numbered medium-chain fatty acids since oxidation of heptanoate yields both two molecules of acetyl-CoA and a molecule of propionyl-CoA. This odd-numbered fatty acid ester cannot be further β -oxidized, but it can be converted into succinyl-CoA and enter the Krebs cycle as an anaplerotic compound. Succinyl-CoA enters the Krebs cycle downstream of isocitrate dehydrogenase 2/3 (IDH2/3). IDH2/3 are rate-limiting Krebs cycle reactions and bypassing these explains the high anaplerotic potential of propionyl-CoA formed from heptanoate, together with the thermodynamically highly favoured formation of succinate from succinyl-CoA [23,28,29]. IDH2 is generally considered a central contributor to the mitochondrial matrix NADPH pool and hence GSH replenishment [17,18,30]. Therefore, bypassing of IDH2-dependent NADPH production could affect the ability of heptanoate to fuel the mitochondrial antioxidant defence system and affect the capacity of heptanoate to protect against myopathic events in patients with VLCAD deficiency.

The ability of medium-chain fatty acids to protect against metabolic stress-induced GSH depletion in VLCAD-deficient cells has not previously been investigated. In the present study, we modified a previously published metabolic stress protocol to test the ability of odd- or even-numbered medium-chain fatty acids to protect against GSH depletion

in VLCAD-deficient patient cells during metabolic stress.

2. Materials and methods

2.1. Patient and control dermal fibroblasts

Dermal fibroblast cell lines derived from patients, diagnosed with mild ($n = 3$) or severe ($n = 3$) VLCAD deficiency based on clinical presentation, abnormal acyl-carnitines and biallelic pathogenic VLCAD variations, were used in this study. VLCAD-deficient dermal fibroblast cell lines were anonymised as per the instructions of the Danish National Committee on Health Research Ethics. The anonymised VLCAD-deficient cell lines were subsequently assigned abbreviations, as seen below in Table 1. Commercial healthy control dermal fibroblast cell lines were also used ($n = 3$). Laboratory validation data for patient fibroblasts have previously been published [15].

2.2. Cell culturing and metabolic stress model

The human dermal fibroblast cell lines were cultured under standard conditions in a CO₂ incubator. Fibroblast cell lines used for assays were kept below 14 passages and were routinely checked for mycoplasma. For all experiments, we used Minimum Essential Media (MEM) (Lonza, Switzerland), which was supplemented with 10%v/v foetal bovine serum (Invitrogen, USA), and 0.1%v/v penicillin & streptomycin (Sigma-Aldrich, Germany).

We wanted to study the effect of various anaplerotic compounds during metabolic stress using a previously published stress protocol [15,16], modified as described below. To control for the two most abundant sources of anaplerotic compounds in complete media, glucose and glutamine [30–34], all experiments were performed at the standard MEM glucose concentration of 5.6 mM corresponding to normal fasting blood glucose levels. L-Glutamine (Gln) final concentration was either 1 mM or 5 mM. 5 mM Gln is the standard supra-physiological concentration used in most cell culture studies [34]. The cultures grown with 1 mM Gln were further supplemented with 0 μ M, 1 μ M, 10 μ M or 100 μ M heptanoate (Sigma-Aldrich, Germany) or octanoate (Sigma-Aldrich, Germany). For the bezafibrate (Sigma-Aldrich, Germany) pretreated cells, bezafibrate was solubilised in dimethyl sulfoxide (Sigma-Aldrich, Germany), and a 400 μ M final concentration was used [19].

During pre-treatment, cells were cultured for 96 h (h) with any of the specific media compositions, in order to allow sufficient time for the individual cell lines to adapt to substrate-induced alterations of the cellular phenotype. During this period, media were replaced every 24 h with media of the same composition. All cells were reseeded during this pretreatment period so that the cultures were 80 % confluent when harvested for assays.

Table 1

Patients' acyl-CoA dehydrogenase very-long chain (ACADVL) genotypes and study ID.

Patient cell lines	ID	Acyl-CoA Dehydrogenase Very Long-Chain (ACADVL) genotype	
		cDNA	Protein
Mild phenotype patient 1	M1	c.[848T>C];[848T>C]	p.[Val283Ala];[Val283Ala]
Mild phenotype patient 2	M2	c.[689C>T];[428_467del40bp]	p.[Thr230Ile];[Gly143Alafs*61]
Mild phenotype patient 3	M3	c.[685C>T];[685C>T]	p.[Arg229*];[Arg229*]
Severe phenotype patient 1	S1	c.[799_802del4bp];[799_802del4bp]	p.[Val267Glnfs*8];[Val267Glnfs*8]
Severe phenotype patient 2	S2	c.[65C>A];[65C>A]	p.[Ser22*];[Ser22*]
Severe phenotype patient 3	S3	c.[848T>C];[864C>T]	p.[Val283Ala];[Phe288=]

Sequence data are based on NM_000018.3.

For the metabolic stress assays, cell lines were pretreated as above with specific media compositions for 96 h. The specific culture media was then replaced one final time (metabolic stress $t = 0$ h), and the cell cultures were transferred to a 41 °C incubator for 96 h without further media changes (Fig. 1).

2.3. Spectrophotometric enzyme assays

Spectrophotometric measurements of mitochondrial respiratory complex I, mitochondrial respiratory complex II/III and citrate synthase (CS) activity were performed on an Uvikon XS spectrometer, as published previously [35]. Fibroblasts were cultured in MEM supplemented with 5 mM Gln, 1 mM Gln + 100 μ M C7 or 1 mM Gln + 100 μ M C8 for 96 h prior to the harvest of assay sample. The results represent data from at least two independent culture replicates of individual cell lines, that were 80–90 % confluent when harvested.

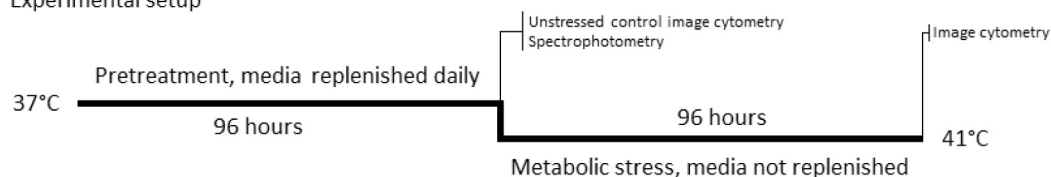
Complex I activity was calculated from the rate of reduction of NADH at 340 nm. Nonspecific activity was removed by subtracting rotenone insensitive activity from total measured activity [36,37]. Mitochondrial respiratory complex II/III activity was calculated from the rate of reduction of cytochrome C at 550 nm in a potassium phosphate buffer. Nonspecific activity was removed by subtracting Antimycin A insensitive activity from total measured activity [37,38]. CS catalyses the condensation of oxaloacetate and acetyl-CoA to citrate and CoA-SH. A coupled reaction of CoA-SH with 5,5'-dithiobis-2-nitrobenzoic acid leads to the formation of 2-nitro-5-thiobenzoate, which is measurable at 412 nm. Each calculated activity was normalised to total protein concentration, measured by Lowry assay [39]. All spectrophotometric reagents were purchased from Sigma-Aldrich, Germany.

2.4. Image cytometry

Assays were performed in A2-slides on a NucleoCounter 3000 (ChemoMetec, Denmark), using trypsinised cells from 80 to 90 % confluent dermal fibroblast cultures. Every assay measured at least 5000 individual cells, allowing robust normalisation of data to mean fluorescence intensity. Presented data represent at least three independent culture replicates of individual cell lines. When seeding cells, total and viable cells were measured by analysing fibroblasts in solution immediately after addition of 4',6-Diamidino-2-phenylindole (DAPI) for non-viable cell concentration and with addition of lysis buffer for total cell concentration.

Intracellular glutathione (GSH) and total thiols were measured with the cell permeable probes Vitabright43 and Vitabright48, respectively (ChemoMetec, Denmark) [40,41]. For all GSH measurements, the NucleoCounter 3000 Darkfield option was used to identify individual cells and RedDot2 (Biotium, USA) was used as a dead cell stain. Vitabright43 was used at 1:200 final dilution and RedDot2 at a 1:1000 final dilution. Vitabright43 fluorescence was detected using peak excitation at 365 nm and emission at 470 nm. RedDot2 fluorescence was detected using peak excitation at 630 nm and emission at 740/60 nm. As a positive control, we inhibited the rate-limiting step of GSH synthesis for 16

Experimental setup



treatment. Media were renewed with preheated media and transferred to a 41 °C incubator without further media renewal for 96 h (fasting). Krebs cycle and OXPHOS activities were measured by spectrophotometric analysis at the end of the pretreatment period, the image cytometry assays (GSH, thiols, viability) at basal 5 mM Gln unstressed conditions were also performed at this time point. The remaining image cytometry measurements of GSH, thiols and viability were performed after 96-h of heat stress.

h using 0.5 mM l-buthionine sulphoximine (BSO) (Sigma-Aldrich, Germany), which removed the majority of the GSH probe (Vitabright43), signal as previously described [41].

For all measurements of total thiols, acridine orange (AO) (ChemoMetec, Denmark) was used to identify individual cells and propidium iodide (PI) (ChemoMetec, Denmark) was used as a dead cell stain. Final concentrations used were Vitabright48 20 mg/mL, AO 0.06 mg/mL and PI 25 mg/mL. Vitabright48 fluorescence was detected using peak excitation at 365 nm and emission at 455 nm. AO fluorescence was detected using peak excitation at 475 nm and emission at 560/35 nm, and PI fluorescence was detected using peak excitation at 530 nm and emission at 675/75 nm.

2.5. Statistical analysis

The spectrophotometric data were imported into Microsoft Excel to calculate enzymatic rates. Image cytometry data were analysed using NucleoView™ software (ChemoMetec, Denmark); the procedures have been described previously in [16]. Graph preparation was performed using the Graphpad Prism 9.1.1 software package (USA), which was also used to calculate standard deviation (SD) and standard error of the mean (SEM), two-way ANOVA and Fisher's least significant difference (LSD) test; P -values <0.05 were considered significant.

3. Results

3.1. Effects of medium-chain fatty acids on mitochondrial bioenergetic capacity

Before comparing the ability of odd- and even-numbered medium-chain fatty acids to power antioxidant capacity in VLCAD-deficient cells, we assayed some basic components of mitochondrial bioenergetics. Using two-way ANOVA, we found that VLCAD-deficient patient cells have decreased CS activity compared with healthy controls, even when glutamine (Gln) was added to culture media as an anaplerotic compound at standard culture concentrations (5 mM). Interestingly, partially replacing Gln as anaplerotic substrate with 100 μ M heptanoate (C7) or octanoate (C8) (and lowering Gln to 1 mM) for 96 h increased the mean CS capacity in both mild and severe patient cells to control levels (Fig. 2B, individual cell line measures in Fig. 2A).

We next analysed respiratory chain complex activities. When compared with the group of healthy control cell lines at standard 5 mM Gln conditions, the group of cell lines derived from mild VLCAD-deficient patients had higher mean activities of respiratory chain complex I and complex II/III, both reaching significant higher levels upon treatment with C7 or C8. By contrast, respiratory chain complex I and II/III activities in cell lines derived from patients with severe VLCAD deficiency did not differ from those of healthy controls at standard conditions and did not increase upon treatment with C7 or C8 (Fig. 2D and F, individual cell line measures in Fig. 2C and E). These data suggest that medium-chain fatty acids increase the uptake capacity of acetyl-CoA into the Krebs cycle, and that a concurrent increase in respiratory

Fig. 1. Experimental setup.

Cells were cultivated at 37 °C in MEM supplemented with various concentrations of glutamine, heptanoate, or octanoate for a period of 96 h (pretreatment), with a daily renewal of culture media with the same composition of glutamine and fatty acids. Cells were reseeded after 72 h. Heat stress was initiated after 96 h pretreatment.

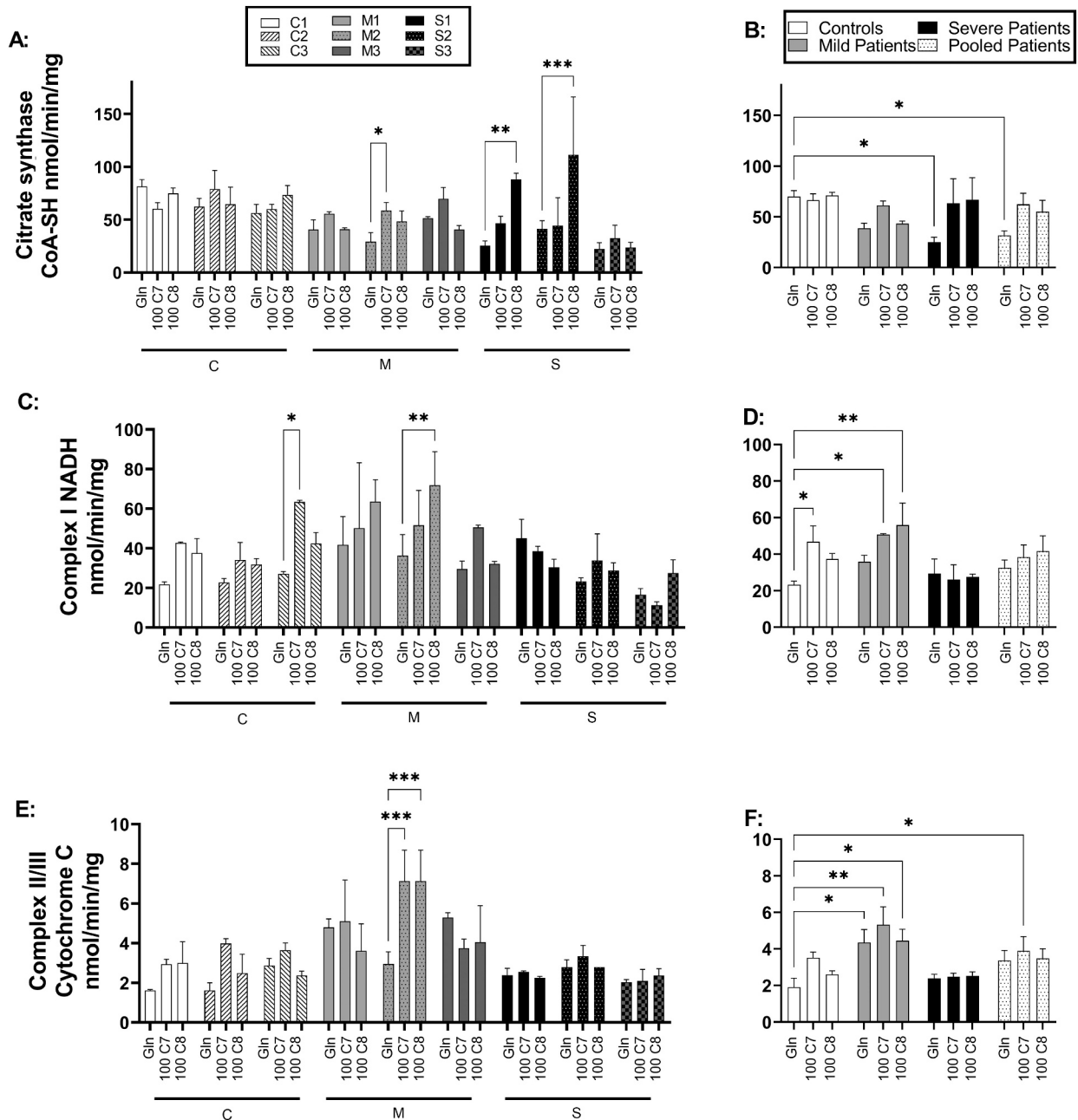


Fig. 2. Mitochondrial bioenergetic enzyme capacity.

The graphs show photospectrometry results from dermal fibroblasts from three control (C1-C3), three mild phenotype (M1-M3) and three severe phenotype (S1-S3) donors. Culture conditions are abbreviated as follows: Gln: 5 mM glutamine, 100 C7: 1 mM glutamine + 100 μM heptanoate, 100 C8: 1 mM glutamine + 100 μM octanoate. Krebs cycle enzyme citrate synthase (CS) maximum activity (CoA-SH(nmol/min)/mg protein) data are displayed as: (A) CS for individual cell line means ± SD of 2 experimental replicates and (B) CS for group means ± SEM of 3 different cell lines of the same genotype class. Mitochondrial respiratory chain complex I (CI) maximum activity data (NADH(nmol/min)/mg total protein) are displayed as: (C) CI for individual cell line means ± SD of 2 experimental replicates and (D) CI for group means ± SEM of 3 different cell lines of the same genotype class. Respiratory chain complex II/III (CII/III) maximum activity data (cytochrome c(nmol/min)/mg total protein) are displayed as: (E) CII/III for individual cell line means ± SD of 2 experimental replicates and (F) CII/III for group means ± SEM of 3 different cell lines of the same genotype class. Fishers LSD significant differences (**P* < 0.05, ***P* < 0.01, ****P* < 0.001) are displayed for individual cell lines as control media (Gln) versus remaining conditions (A, C, E), and for group means of the same genotype class as controls (Ctrl) versus remaining conditions (B, D, F).

chain complex activities takes place in mild phenotype cell lines but not in severe phenotypes cell lines.

3.2. Medium-chain fatty acids rescue cataplerotic stress induced GSH depletion in VLCAD-deficient cells

We have recently shown that metabolic stress affects the capacity of VLCAD-deficient patient cells to cope with oxidative stress by decreasing

the GSH antioxidant defence capacity [15,16]. Moreover, increased metabolic stress during prolonged exercise aggravated cataplerotic stress and decreased Krebs cycle intermediates in the VLCAD-deficient mice model [21]. It is not known if even- or odd-numbered medium-chain fatty acids can provide protection against antioxidant depletion and oxidative damage in VLCAD-deficient cells during metabolic stress. In order to test this, we used a cataplerotic, heat stress model, modified from our previous work, where cells were pretreated with various media

types for 96 h and subsequently exposed to 96 h of metabolic heat stress before measurements of antioxidant capacity (see Fig. 1 and Materials and methods).

In a previous version of this metabolic stress model, we found that standard culture conditions with 5.6 mM glucose and 5 mM Gln enabled VLCAD-deficient fibroblast to retain GSH levels. The VLCAD-deficient cell lines did however experience an increased oxidative stress burden that may act as a form of cataplerotic stress as the different cellular compartments have to redirect a larger amount of reducing equivalents

to the formation of NADPH to power the antioxidant systems [15]. Gln acts as a primary anaplerotic substrate under standard cell culture conditions, and a significant reduction of Gln decreases anaplerotic capacity or causes cataplerotic stress [31,34,42,43].

Two-way ANOVA found that reducing the Gln concentration to 1 mM before subjecting VLCAD-deficient fibroblasts to metabolic stress had a significant effect on their ability to maintain cellular GSH levels. As compared with unstressed conditions, the 1 mM Gln culturing condition led to significant decreases in mean GSH levels in the mild and severe

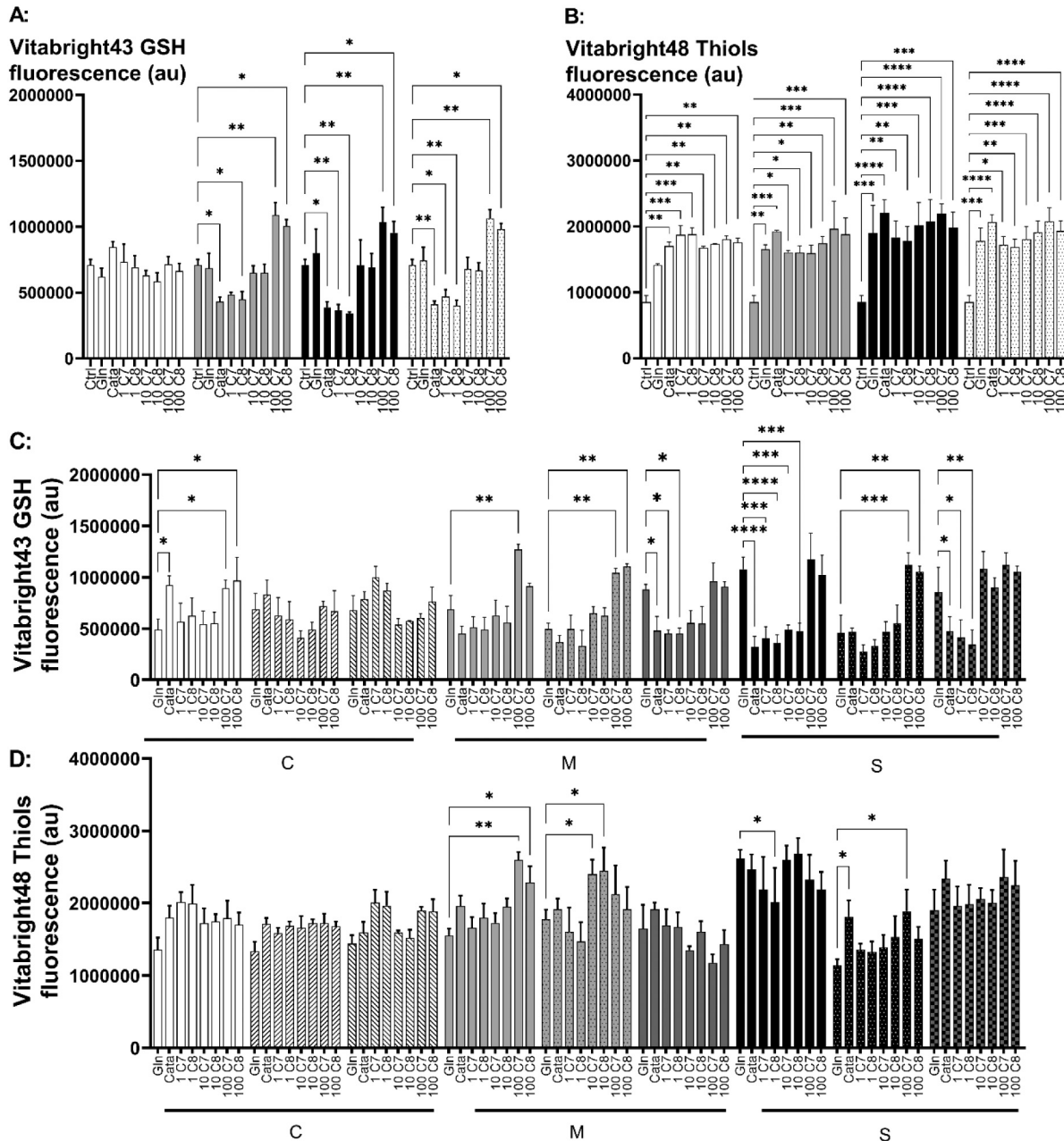


Fig. 3. Cataplerotic stress effect on thiols.

The graphs show image cytometry mean fluorescence intensity from dermal fibroblast cell lines from three control (C1-C3), three mild phenotype (M1-M3) and three severe phenotype (S1-S3) donor. Cells were pretreated with various media types for 96 h and subsequently exposed to fasting heat stress for 96 h. Culture conditions are abbreviated as follows: Ctrl: untreated control fibroblasts without exposure to fasting heat stress, Gln: 5 mM glutamine, Cata: 1 mM glutamine, 1 C7: 1 mM glutamine + 1 μM heptanoate, 1 C8: 1 mM glutamine + 1 μM octanoate, 10 C7: 1 mM glutamine + 10 μM heptanoate, 10 C8: 1 mM glutamine + 10 μM octanoate, 100 C7: 1 mM glutamine + 100 μM heptanoate, 100 C8: 1 mM glutamine + 100 μM octanoate. (A): Glutathione (GSH), (B): Total thiol group means, error bars ± SEM of 3 different cell lines of the same genotype class. Fishers LSD significant differences (* $P < 0.05$, ** $P < 0.01$, *** $P < 0.001$) are shown for each media type compared with untreated controls (Ctrl). (C): Individual cell lines levels of GSH and (D): total thiols, error bars ± SD of 3 experimental replicates. Fishers LSD significant differences (* $P < 0.05$, ** $P < 0.01$, *** $P < 0.001$) are shown for each media type, compared with 5 mM glutamine treatment.

VLCAD-deficient cell line groups but not in the control group. Addition of 1 μ M C7 or C8 did not alter this outcome. However, 10 and 100 μ M C7 or C8 increased GSH levels to untreated control levels or above (Fig. 3A, individual cell line measures shown in 3C).

This GSH depletion could potentially be related to ongoing depletion of thiols or cell death. To test this, we first measured total thiols. In both patient and control cell line groups, metabolic stress led to a near doubling of mean thiol intensity levels compared with unstressed control conditions, regardless of media composition (Fig. 3B, individual cell line measures shown in 3D). During metabolic stress, both patient groups, but not the group of healthy controls, showed a slight but significant decrease in mean viability when cultured at 1 mM Gln, but not 5 mM Gln, as compared with unstressed conditions. Treatment with media containing 1 mM Gln plus 100 μ M C7 or 1 mM Gln plus 100 μ M C8 corrected the decreased viability (Fig. 4B, individual cell line measures shown in Fig. 4A).

3.3. Medium-chain fatty acids protects against the additive effects on GSH depletion of PPAR overactivation and cataplerotic stress

We have previously found that peroxisome proliferator-activated receptor (PPAR) overactivation, induced by culturing VLCAD-deficient fibroblast with 400 μ M bezafibrate prior to metabolic stress, led to enhanced GSH depletion and an eventual decrease in cellular viability

[15]. Chronic overactivation of PPAR in vivo is a concern in VLCAD deficiency because the accumulated long-chain fatty acid metabolites are potent PPAR agonists [5,15]. To mimic this overactivation, we repeated the metabolic stress assays above, but in the presence of the PPAR agonist bezafibrate. 400 μ M bezafibrate cotreatment resulted in 5 mM Gln, 1 mM Gln plus 10 μ M C7 or 1 mM Gln plus 10 μ M C8 being insufficient to protect any of the VLCAD-deficient cell line groups from GSH depletion. However, 100 μ M C7 or C8 was sufficient to preserve or increase GSH levels in both patient groups (Fig. 5A, individual cell line measures shown in 5C). Under the same stress conditions, both the control and patient cell lines increased total thiol levels and were capable of maintaining total thiol levels, even in the treatment condition with reduced Gln and in the absence of medium-chain fatty acids (Fig. 5B, individual cell line measures are shown in 5D). When testing the viability of VLCAD-deficient cell lines, we found that both VLCAD-deficient cell line groups had a significant decrease in viability when cultured with 1 mM Gln or with 1 μ M C7 or C8. The 10 μ M dosage of each medium-chain fatty acids was, however, sufficient to protect against the decrease in viability (Fig. 6A, individual cell line measures shown in 6B).

Overall, an additive effect of the stress imposed by PPAR overactivation via bezafibrate and cataplerotic stress with 1 mM Gln was observed, with the combined effect resulting in a further >10 % decrease in GSH depletion (Figs. 3A and 5A) and viability (Figs. 4B and

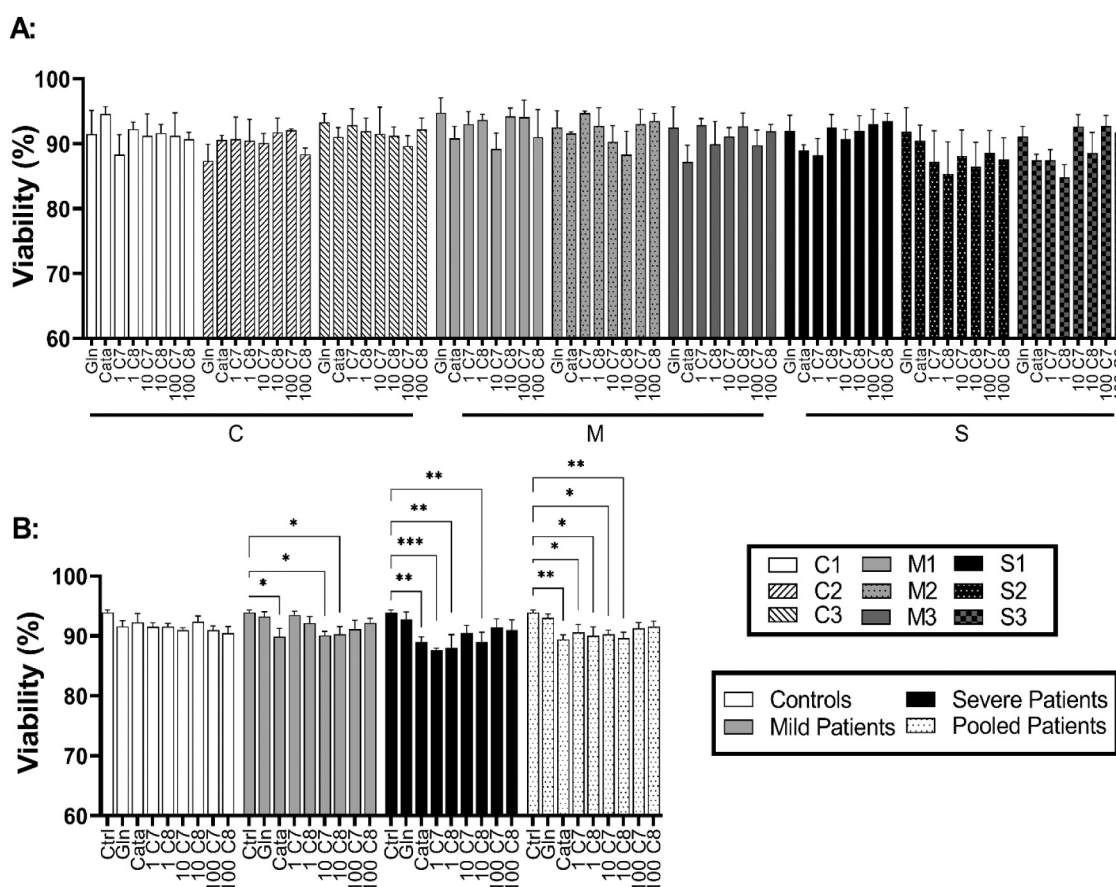


Fig. 4. Cataplerotic stress effect on viability.

The graphs show image cytometry measured viability in dermal fibroblast cell lines from three control (C1-C3), three mild phenotype (M1-M3) and three severe phenotype (S1-S3) donors. Cells were pretreated with various media types for 96 h and subsequently exposed to fasting heat stress for 96 h. Culture conditions are abbreviated as follows: Ctrl: untreated control fibroblasts without exposure to fasting heat stress, Gln: 5 mM glutamine, Cata: 1 mM glutamine, 1 C7: 1 mM glutamine+1 μ M heptanoate, 1 C8: 1 mM glutamine + 1 μ M octanoate, 10 C7: 1 mM glutamine + 10 μ M heptanoate, 10 C8: 1 mM glutamine + 10 μ M octanoate, 100 C7: 1 mM glutamine + 100 μ M heptanoate, 100 C8: 1 mM glutamine + 100 μ M octanoate. (A): Individual cell lines' viability (%), error bars \pm SD of 3 experimental replicates. Fishers LSD significant differences (* P < 0.05, ** P < 0.01, *** P < 0.001) are shown for each media type, compared with 5 mM glutamine treatment. (B): Percentage viable cells, error bars \pm SEM of 3 different cell lines of the same genotype class. Fishers LSD significant differences (* P < 0.05, ** P < 0.01, *** P < 0.001) are shown for each media type, compared with untreated controls (Ctrl).

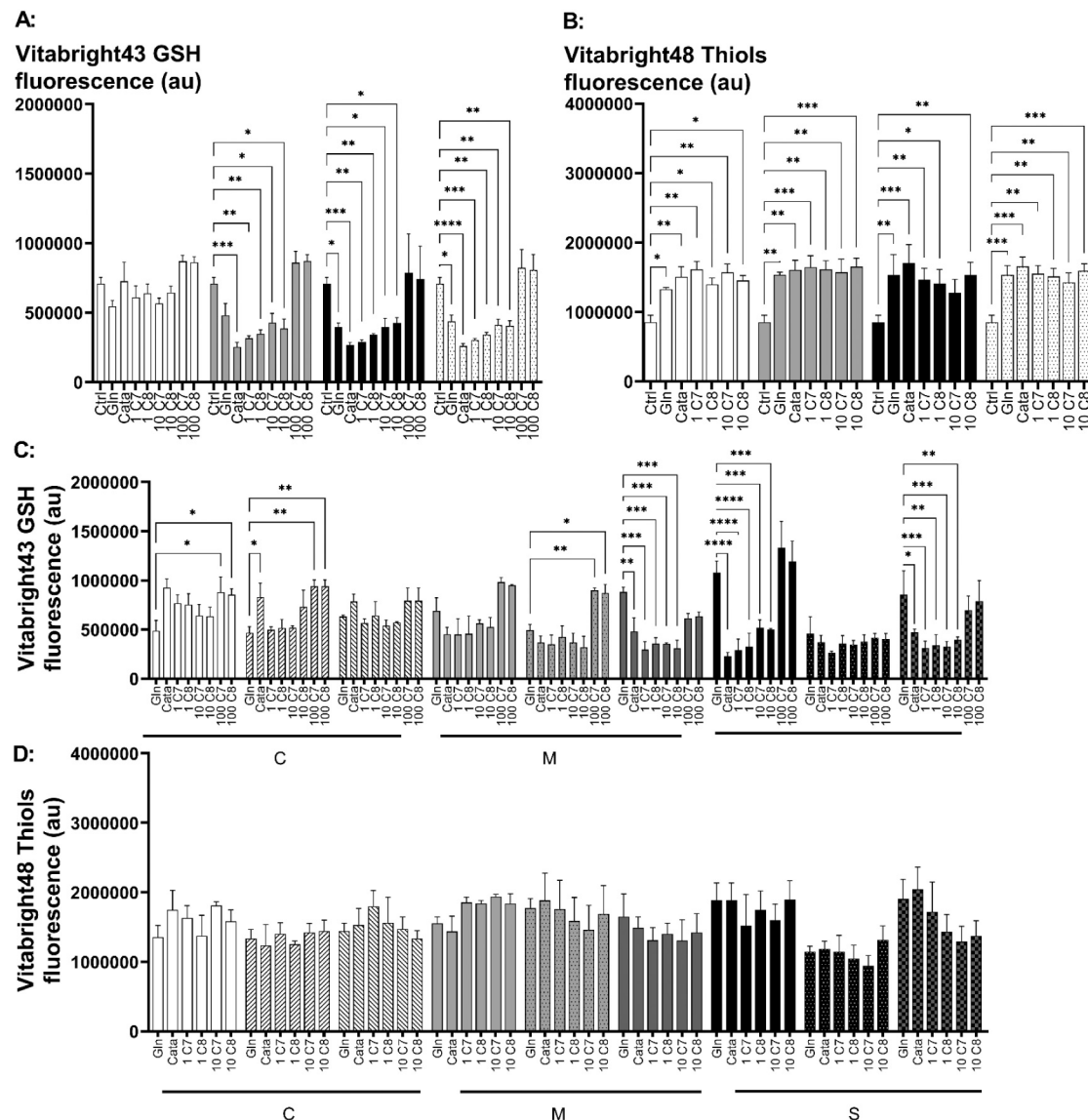


Fig. 5. Cataplerotic stress and bezafibrate effect on thiols.

The graphs show image cytometry mean fluorescence intensity from dermal fibroblast cell lines from three control (C1-C3), three mild phenotype (M1-M3) and three severe phenotype (S1-S3) donors. Cells were pretreated with 400 μ M bezafibrate and various concentrations of glutamine and medium-chain fatty acids for 96 h, abbreviated as follows: Ctrl: untreated control fibroblasts without exposure to fasting heat stress, Gln: 5 mM glutamine, Cata: 1 mM glutamine, 1 C7: 1 mM glutamine + 1 μ M heptanoate, 1 C8: 1 mM glutamine + 1 μ M octanoate, 10 C7: 1 mM glutamine + 10 μ M heptanoate, 10 C8: 1 mM glutamine + 10 μ M octanoate, 100 C7: 1 mM glutamine + 100 μ M heptanoate, 100 C8: 1 mM glutamine + 100 μ M octanoate. Subsequently cells were exposed to fasting heat stress for 96 h. (A): Glutathione (GSH) and (B): total thiols group means \pm SEM of 3 different cell lines of the same genotype class. Fishers LSD significant differences (* P < 0.05, ** P < 0.01, *** P < 0.001) are shown for each media type compared with untreated controls (Ctrl). (C): Individual cell lines levels of GSH and (D) total thiols \pm SD of 3 experimental replicates. Fishers LSD significant differences (* P < 0.05, ** P < 0.01, *** P < 0.001) are shown for each media type, compared with 5 mM glutamine treatment.

6B) compared with the cataplerotic stress alone.

4. Discussion

We have previously shown that redox homeostasis and defence against oxidative stress are compromised in VLCAD-deficient cells and that exposure to external metabolic stress can cause increased ROS production and GSH depletion [15,16], supporting the general finding that the development of chronic VLCAD deficiency symptoms are strongly associated with oxidative stress and antioxidant function [5,12,14,44–47].

It has previously been shown that inability to oxidise sufficient long-chain fatty acids can induce cataplerotic stress and energy shortage and negatively affect other essential aspects of mitochondrial metabolism,

such as the maintenance of the NAD(P)H pool in the mitochondrial matrix [12,21]. In this article, we find evidence that medium-chain fatty acids can rescue VLCAD-deficient cells from GSH depletion induced by cataplerotic stress and from the negative effects induced by the combined cataplerotic stress and PPAR overactivation via bezafibrate, in a dose dependent-manner. The study is summarized in Fig. 7.

4.1. Effect of medium-chain fatty acids on bioenergetic capacity

While medium-chain fatty acids increased CS activity in both patient groups compared with that of healthy control levels, the results for respiratory chain complex I and II/III activities were more variable. Complex I and II/III activities increased after treatment with medium-chain fatty acids in both healthy controls and the group of mild

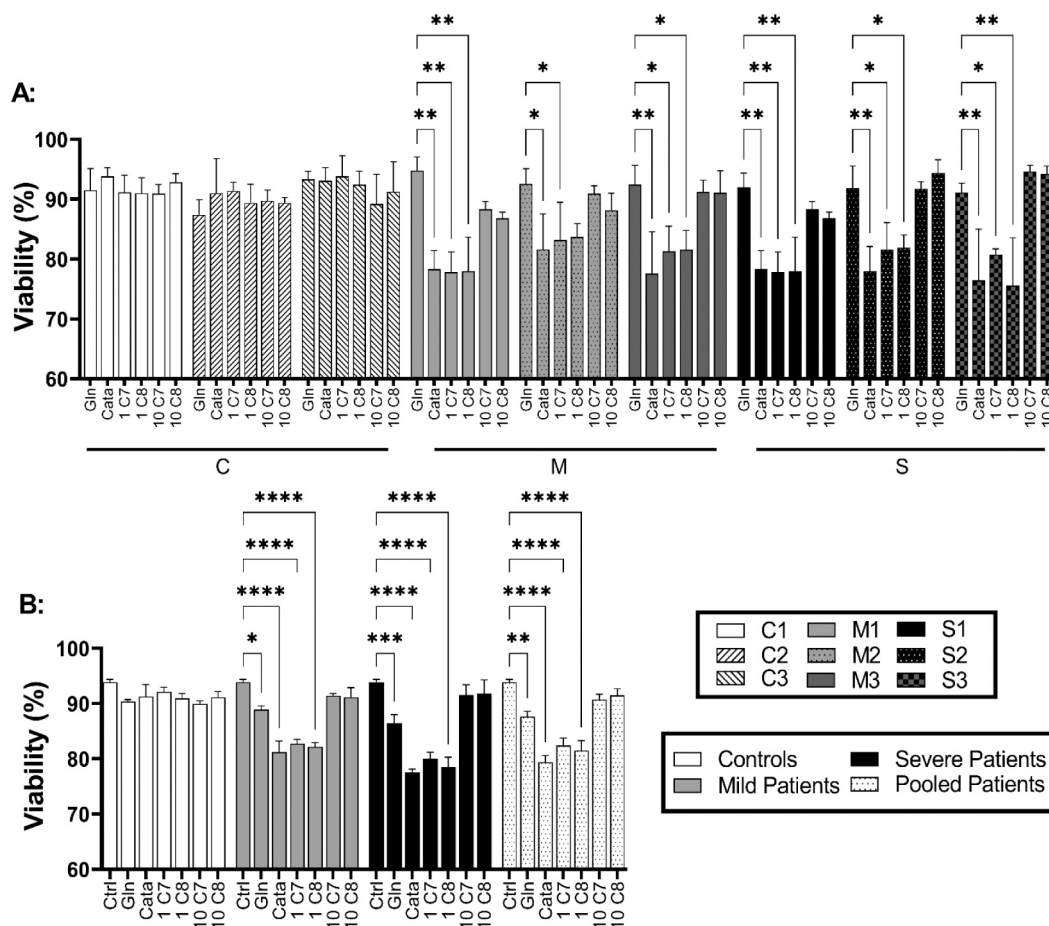


Fig. 6. Cataplerotic stress and bezafibrate effect on viability.

The graphs show image cytometry measured viability in dermal fibroblast cell lines from three control (C1-C3), three mild phenotype (M1-M3) and three severe phenotype (S1-S3) donors. Cells were pretreated with 400 μ M bezafibrate and various concentrations of glutamine and medium-chain fatty acids for 96 h and subsequently exposed to fasting heat stress for 96 h. Culture conditions are abbreviated as follows: Ctrl: untreated control fibroblasts without exposure to fasting heat stress, Gln: 5 mM glutamine, Cata: 1 mM glutamine, 1 C7: 1 mM glutamine + 1 μ M heptanoate, 1 C8: 1 mM glutamine + 1 μ M octanoate, 10 C7: 1 mM glutamine + 10 μ M heptanoate, 10 C8: 1 mM glutamine + 10 μ M octanoate, 100 C7: 1 mM glutamine + 100 μ M heptanoate, 100 C8: 1 mM glutamine + 100 μ M octanoate. (A): Individual cell lines percentage viable cells \pm SD of 3 experimental replicates. Fishers LSD significant differences ($*P < 0.05$, $**P < 0.01$) is shown for each media type, compared with 5 mM glutamine treatment. (B) Mean viability \pm SEM of 3 different cell lines of the same genotype class. Fishers LSD significant differences ($*P < 0.05$, $**P < 0.01$, $***P < 0.001$, $****P < 0.0001$) are shown for each media type, compared with untreated controls (Ctrl).

phenotype cell lines but not in the severe phenotype cell lines. The data indicate that control and mild phenotype cell lines might have bioenergetically enzymatic systems that are more flexible with regard to altering spare capacity than severe phenotype cell lines.

Supplying substrates that bypass the metabolic block in VLCAD-deficient cells could reduce the oxidative burden by supporting matrix NADPH production for GSH replenishment, thereby reducing the vicious cycle by which persistent mitochondrial oxidative damage leads to increased ROS production and impaired bioenergetics capacity. Previously, mitochondrial antioxidants have been shown to improve mitochondrial bioenergetic capacity in VLCAD-deficient cells [14]. We were therefore surprised not to find persistent bioenergetic improvements in the VLCAD-deficient cells upon treatment with medium-chain fatty acids. This lack of effect could simply be a result of insufficient treatment time. Alternatively, it may reflect the limitations of the indirect antioxidant effect of medium-chain fatty acids treatment in VLCAD-deficient cells as opposed to using actual mitochondrial targeted antioxidants, as discussed further below.

4.2. Effect of medium-chain fatty acids on antioxidant function

Applying cataplerotic heat stress to control cell lines did not affect

their ability to retain GSH levels. The ability of control cell lines to retain GSH levels can probably be ascribed to the fact that control cell lines have a significantly lower oxidative burden than VLCAD-deficient cells [15]. In addition, control fibroblasts possess a normal long-chain FAO capacity that can be used to oxidise endogenously released long-chain fatty acids for ATP and NADPH production [15,16,48,49].

We found that cataplerotic stress depleted GSH levels in patient cell lines and that depletion of GSH could be rescued by the addition of medium-chain fatty acids in a dose-dependent manner. It is important to measure whole cell GSH and total thiol levels when evaluating GSH depletion, also when this depletion is due to oxidative stress originating in the mitochondria. GSH is synthesized only in the cytosol and is actively imported into the mitochondria. The mitochondria in turn produce most of the cellular ROS. Combined, this means that mitochondria can function as a GSH sink and that mitochondrial GSH levels can remain high, while the cytosol is becoming GSH-depleted, until an apoptotic threshold is reached or the mitochondria become dysfunctional and oxygen consumption rates drop [15,50,51].

In line with our previous study [15], we found that while the signal from the probe targeting reduced GSH (Vitabright43) diminished in patient cell lines during metabolic stress exposure, the same stress led to an increase in the signal from the probe targeting the total pool of

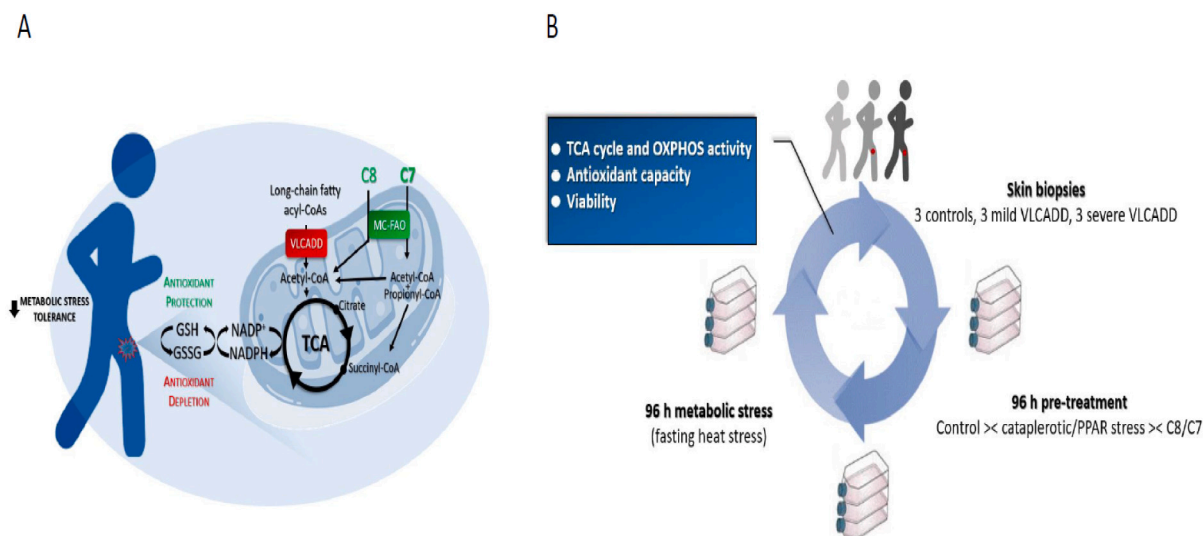


Fig. 7. Summary of results.

Previous studies have shown that VLCAD deficient patients have a decreased tolerance for metabolic stress, which may result in aggravation of cataplerotic stress with energy and antioxidant depletion during prolonged exercise or fasting. (A) Here, we hypothesize that odd- or even-numbered medium-chain fatty acids (C8 or C7) can provide protection against antioxidant depletion and increase metabolic stress tolerance in VLCAD deficiency. (B) To test this hypothesis, we mimicked the in vivo situation by applying chronic metabolic stress to control and patient cells in culture and tested if even- or odd-numbered medium-chain fatty acids (C7 or C8) could provide protection against antioxidant depletion and decreased cellular viability in VLCAD deficient cells. We found that metabolic stress led to antioxidant depletion in VLCAD-deficient cell lines (outcome coloured red) and that medium-chain fatty acids could protect against antioxidant depletion during metabolic stress (outcome coloured green).

reduced thiols (Vitabright48). This signal increase was of a uniform size in control, mild, and severe patient cell lines compared with untreated controls. Gln and medium-chain fatty acid concentration did not change this outcome, nor did the presence of the PPAR agonist bezafibrate. More work is required to explain this finding, but we speculate that the increased Vitabright48 signal is due to increased thiol uptake by the cell from the media or increased exposure of protein-bound thiol groups. The former would be due to an attempt to increase GSH production, as a compensatory cellular mechanism for the increased oxidative burden. The latter would be due to partial protein denaturing caused by heat stress.

GSH is the most abundant small-molecule thiol in solution, but the cellular cysteine pool, intermediates of GSH synthesis and other small-molecule thiols, such as cysteamine, constitute quite large fractions of the GSH pool [52,53]. The exposed thiol groups on protein surfaces are larger than the GSH pool. For instance, the concentration of exposed protein thiol groups in healthy liver tissue is approximately 25-fold higher than total GSH levels, and approximately 40-fold higher in healthy heart tissue [54]. This explains the low sensitivity of the total thiol probe Vitabright48 to partial GSH depletion induced by BSO treatment and GSH depletion induced by metabolic stress, as previously published [15,41]. Partial protein denaturing would seem to be the most likely explanation, considering that the pool of protein-bound thiols is larger than the pool of small-molecule thiols and that the heat stressed controls experience an increased total thiol signal, but no GSH depletion and little additional oxidative burden [15].

Heptanoate was not superior to octanoate as a fuel for powering the antioxidant system, which is somewhat surprising considering that clinical studies of VLCAD-deficient patients as well as studies of the VLCAD-deficient mouse show that heptanoate, as compared with octanoate, has an increased capacity to improve clinical outcome, decrease cataplerotic stress and increase Krebs cycle intermediates [25,26,55–57].

One possible explanation is that the cataplerotic stress is too mild or the concentrations of other anaplerotic substrates (glucose and glutamate) are too high in the culture media, for the propionyl-CoA groups from heptanoate to be required. This is, however, unlikely, as the degree

of GSH depletion is similar across the different concentration ranges of heptanoate and octanoate.

Alternatively, heptanoate, in contrast to octanoate, partially bypasses Krebs cycle IDH2, which is a major contributor to the matrix NADPH pool. This could negate the ability of odd-chain fatty acids to better fuel the matrix antioxidant system despite a superior anaplerotic profile compared with even-numbered, medium-chain fatty acids [17,18]. Further studies would be required to draw more detailed conclusions.

4.3. Implications for the clinical effect of triheptanoin

We found that both types of medium-chain fatty acids protect in a similar manner against antioxidant depletion, induced by a combination of fasting heat stress, PPAR overactivation and cataplerotic stress.

If this is also true in vivo, this leads to two potential explanations for the myopathic symptoms that persist following clinical trials of triheptanoin [9,58,59]. One is that oxidative stress is not an important or sole pathogenic factor for the myopathic phenotype. Another is that insufficient quantities of medium-chain fatty acids are delivered to the skeletal muscle.

As to the first theory, it seems quite reasonable that oxidative stress is not the sole pathogenic factor. For example, toxic levels of long-chain fatty acids and their metabolites are known to accumulate and could be important drivers of the myopathic phenotype, for instance by disruption of cellular membrane structures. In addition, treatment with odd- or even-numbered medium-chain fatty acids results in accumulation of different elongated fatty acids and more complex lipid species. The long-term effect of this in VLCAD-deficient patients is essentially unknown, but complex lipids with a significant potential to induce inflammation have been shown to accumulate in VLCAD-deficient patients, regardless of whether the treatment regime is with odd- or even-numbered, medium-chain fatty acids [9,55,57–61]. More research is required to draw further conclusions.

The alternative theory is that bioavailability of the medium-chain fatty acids in skeletal muscle is simply too low. In animal models, orally administered medium-chain triglycerides and triheptanoin are

mostly cleared by hepatic first pass metabolism [61,62]. This explains the abolishment of hypoketotic hypoglycaemic events in clinical trials, since the VLCAD-deficient hepatic tissue has access to plenty of anaplerotic compounds. This improves the flux through the Krebs cycle and electron flow into the respiratory chain, thereby improving the VLCAD-deficient liver's ability to maintain gluconeogenesis [19,61,62]. An unfortunate aspect of the large hepatic consumption of heptanoate is that there will be relatively few heptanoate molecules left to enter the circulation. Any remnant heptanoate and associated beneficial metabolites released by the liver must pass through the heart twice before potentially entering the part of the circulatory system that will eventually make them available to skeletal muscle tissue. It is therefore possible that very few anaplerotic compounds ever reach striated muscle tissues.

This raises the possibility of supplementing oral triheptanoin with odd-numbered, medium-chain fatty acids delivery mechanisms that bypass hepatic first-pass metabolism. Another alternative is treatment with orally available compounds that increase muscle antioxidant capacity, such as treatment with β -alanine leading to increased levels of the highly-muscle specific peptide antioxidant carnosine [62–64]. Alternatively, infusion with the previously discussed mitochondrial targeted antioxidants such as elamipretide is a possibility in VLCAD-deficient patients already metabolically stabilised with triheptanoin [14,65].

5. Conclusions

We conclude that medium-chain fatty acids can power the antioxidant system and protect cellular viability during metabolic stress in VLCAD-deficient patient cells in a dose-dependent manner. As such, the milder myopathic symptoms that remain following clinical trials of triheptanoin in patients with VLCAD deficiency likely cannot be ascribed to an impaired ability of heptanoate to protect against antioxidant depletion. Further studies are required to understand the bioenergetic consequences of an increased GSH antioxidant recycling in VLCAD deficiency and to what extent other pathological features, such as accumulation of long-chain fatty acid metabolites, are important drivers of the myopathic phenotype.

CRedit authorship contribution statement

All authors have read the manuscript and contributed critically.

M.L.: wrote the draft paper, planned the project, and performed the majority of the assays and data analysis.

R. H & I.H.: supervised spectrophotometric assays and guided data analysis.

N. G. & R. K. J. O planned and supervised the project and applied for funding.

Declaration of competing interest

The authors declare the following financial interests/personal relationships which may be considered as potential competing interests: The study was partially funded by Ultragenyx Pharmaceutical Inc., CA, USA without influence on project design and interpretation of data.

Data availability

Data will be made available on request.

Acknowledgments

Aarhus University, Research Unit for Molecular Medicine wishes to thank their colleagues and patient collaborators. Martin Lund wishes to express his gratitude to Ultragenyx Pharmaceutical Inc. CA, USA (Grant ID UX007-IST093) and Aarhus University, Faculty of Health, Graduate School for funding and to Dr. Iain Hargreaves and Robert Heaton for

their great hospitality while hosting him in Liverpool, England.

References

- [1] C. Bertrand, C. Largilliere, M.T. Zabet, M. Mathieu, C. Vianeyssaban, Very long-chain acyl-CoA dehydrogenase-deficiency - identification of a new inborn error of mitochondrial fatty-acid oxidation in fibroblasts, *Biochim. Biophys. Acta* 1180 (3) (1993) 327–329.
- [2] S.M. Houten, S. Violante, F.V. Ventura, R.J.A. Wanders, The biochemistry and physiology of mitochondrial fatty acid β -oxidation and its genetic disorders, *Annu. Rev. Physiol.* 78 (1) (2016) 23–44.
- [3] D. Marsden, C.L. Bedrosian, J. Vockley, Impact of newborn screening on the reported incidence and clinical outcomes associated with medium- and long-chain fatty acid oxidation disorders, *Genet. Med.* 23 (5) (2021) 816–829.
- [4] R.P. McAndrew, Y. Wang, A.-W. Mohsen, M. He, J. Vockley, J.-J.P. Kim, Structural basis for substrate fatty acyl chain specificity: crystal structure of human very long-chain acyl-CoA dehydrogenase, *J. Biol. Chem.* 283 (14) (2008) 9435–9443.
- [5] M. Lund, R.K.J. Olsen, N. Gregersen, A short introduction to acyl-CoA dehydrogenases; deficiencies and novel treatment strategies, *Expert Opin. Orphan Drugs* (2015) 1–12.
- [6] M. Wajner, Alexandre U. Amaral, Mitochondrial dysfunction in fatty acid oxidation disorders: insights from human and animal studies, *Biosci. Rep.* 36 (1) (2016), e00281.
- [7] E.F. Diekman, S. Ferdinandusse, L. van der Pol, H.R. Waterham, J.P. Ruiten, L. Ijlst, R.J. Wanders, S.M. Houten, F.A. Wijburg, A.C. Blank, F.W. Asselbergs, R. H. Houtkooper, G. Visser, Fatty acid oxidation flux predicts the clinical severity of VLCAD deficiency, *Genet. Med.* 17 (12) (2015) 989–994.
- [8] S. Olpin, S. Clark, J. Dalley, B. Andresen, J. Croft, C. Scott, A. Khan, R. Kirk, R. Sparkes, M. Chard, A. Chan, E. Glamuzina, J. Bastin, N. Manning, R. Pollitt, Fibroblast fatty-acid oxidation flux assays stratify risk in newborns with presumptive-positive results on screening for very-long chain acyl-CoA dehydrogenase deficiency, *Int. J. Neonatal Screen.* 3 (1) (2017).
- [9] K. van Eunen, C.M.L. Volker-Touw, A. Gerding, A. Bleeker, J.C. Wolters, W.J. van Rijt, A.-C.M.F. Martines, K.E. Niezen-Koning, R.M. Heiner, H. Permentier, A. K. Groen, D.-J. Reijngoud, T.G.J. Derks, B.M. Bakker, Living on the edge: substrate competition explains loss of robustness in mitochondrial fatty-acid oxidation disorders, *BMC Biol.* 14 (1) (2016) 107.
- [10] P. Laforet, C. Acquaviva-Bourdain, O. Rigal, M. Brivet, I. Penisson-Besnier, B. Chabrol, D. Chaigne, O. Boespflug-Tanguy, C. Laroche, A.L. Bedat-Millet, A. Behin, I. Deleuvaux, A. Lombes, B.S. Andresen, B. Eymard, C. Vianey-Saban, Diagnostic assessment and long-term follow-up of 13 patients with very long-chain acyl-coenzyme a dehydrogenase (VLCAD) deficiency, *Neuromuscul. Disord.* 19 (5) (2009) 324–329.
- [11] E.F. Diekman, G. Visser, J.P.J. Schmitz, R.A.J. Nijelstein, M. de Sain-van, M. der Velden, W.L.Van Wardrop, S.M. der Pol, N.A.W. van Houten, T. Riel, J.A.L. Jeneson Takken, Altered energetics of exercise explain risk of rhabdomyolysis in very long-chain acyl-CoA dehydrogenase deficiency, *PLOS ONE* 11 (2) (2016), e0147818.
- [12] C. Cecatto, A.U. Amaral, J.C. da Silva, A. Wajner, M.D.O.V. Schimit, L.H.R. da Silva, S.M. Wajner, A. Zanatta, R.F. Castilho, M. Wajner, Metabolite accumulation in VLCAD deficiency markedly disrupts mitochondrial bioenergetics and Ca²⁺ homeostasis in the heart, *FEBS J.* 285 (8) (2018) 1437–1455.
- [13] S.M. Houten, H. Herrema, H. te Brinke, S. Denis, J.P.N. Ruiten, T.H. van Dijk, C. A. Argmann, R. Ottenhoff, M. Müller, A.K. Groen, F. Kuipers, D.-J. Reijngoud, R.J. A. Wanders, Impaired amino acid metabolism contributes to fasting-induced hypoglycemia in fatty acid oxidation defects, *Hum. Mol. Genet.* 22 (25) (2013) 5249–5261.
- [14] B. Seminotti, G. Leipnitz, A. Karunanidhi, C. Kochersperger, V.Y. Roginskaya, S. Basu, Y. Wang, P. Wipf, B. Van Houten, A.-W. Mohsen, J. Vockley, Mitochondrial energetics is impaired in very long-chain acyl-CoA dehydrogenase deficiency and can be rescued by treatment with mitochondria-targeted electron scavengers, *Hum. Mol. Genet.* 28 (6) (2018) 928–941.
- [15] M. Lund, K.G. Andersen, R. Heaton, I.P. Hargreaves, N. Gregersen, R.K.J. Olsen, Bezafibrate activation of PPAR drives disturbances in mitochondrial redox bioenergetics and decreases the viability of cells from patients with VLCAD deficiency, *Biochim. Biophys. Acta Mol. basis Dis.* 1867 (6) (2021), 166100.
- [16] P. Fernandez-Guerra, M. Lund, T.J. Corydon, N. Cornelius, N. Gregersen, J. Palmfeldt, P. Bross, in: Application of an Image Cytometry Protocol for Cellular and Mitochondrial Phenotyping on Fibroblasts from Patients with Inherited Disorders, Springer Berlin Heidelberg, 2015, pp. 1–10.
- [17] M. Marí, A. Morales, A. Colell, C. García-Ruiz, N. Kaplowitz, J.C. Fernández-Checa, Mitochondrial glutathione features, regulation and role in disease, *Biochim. Biophys. Acta* 1830 (5) (2013) 3317–3328.
- [18] A. Pedersen, G.B. Karlsson, J. Rydström, Proton-translocating transhydrogenase: an update of unsolved and controversial issues, *J. Bioenerg. Biomembr.* 40 (5) (2008) 463.
- [19] O.E. Owen, S.C. Kalhan, R.W. Hanson, The key role of anaplerosis and cataplerosis for citric acid cycle function, *J. Biol. Chem.* 277 (34) (2002) 30409–30412.
- [20] M. Inigo, S. Deja, S.C. Burgess, Ins and outs of the TCA cycle: the central role of anaplerosis, *Annu. Rev. Nutr.* 41 (1) (2021) 19–47.
- [21] A.J. Bakermans, M.S. Dodd, K. Nicolay, J.J. Prompers, D.J. Tyler, S.M. Houten, Myocardial energy shortage and unmet anaplerotic needs in the fasted long-chain acyl-CoA dehydrogenase knockout mouse, *Cardiovasc. Res.* 100 (3) (2013) 441–449.

- [22] M.B. Gillingham, S.B. Heitner, J. Martin, S. Rose, A. Goldstein, A.H. El-Gharbawy, S. Deward, M.R. Lasarev, J. Pollaro, J.P. DeLany, L.J. Burchill, B. Goodpaster, J. Shoemaker, D. Matern, C.O. Harding, J. Vockley, Triheptanoin versus trioctanoin for long-chain fatty acid oxidation disorders: a double blinded, randomized controlled trial, *J. Inherit. Metab. Dis.* 40 (6) (2017) 831–843.
- [23] H. Brunengraber, C. Roe, Anaplerotic molecules: current and future, *J. Inherit. Metab. Dis.* 29 (2–3) (2006) 327–331.
- [24] J. Vockley, B. Burton, G.T. Berry, N. Longo, J. Phillips, A. Sanchez-Valle, P. Tanpaiboon, S. Grunewald, E. Murphy, A. Bowden, W. Chen, C.-Y. Chen, J. Cataldo, D. Marsden, E. Kakkis, Results from a 78-week, single-arm, open-label phase 2 study to evaluate UX007 in pediatric and adult patients with severe long-chain fatty acid oxidation disorders (LC-FAOD), *J. Inherit. Metab. Dis.* 42 (1) (2019) 169–177, <https://doi.org/10.1002/jimd.12038>.
- [25] J. Vockley, B. Burton, G. Berry, N. Longo, J. Phillips, A. Sanchez-Valle, K. Chapman, P. Tanpaiboon, S. Grunewald, E. Murphy, X. Lu, J. Cataldo, Effects of triheptanoin (UX007) in patients with long-chain fatty acid oxidation disorders: results from an open-label, long-term extension study, *J. Inherit. Metab. Dis.* 44 (1) (2021) 253–263.
- [26] T. Zögeler, K. Stock, M. Jörg-Streller, J. Spenger, V. Konstantopoulou, M. Hufgard-Leitner, S. Scholl-Bürgi, D. Karall, Long-term experience with triheptanoin in 12 Austrian patients with long-chain fatty acid oxidation disorders, *Orphanet J. Rare Dis.* 16 (1) (2021), 28–28.
- [27] J. Vockley, D. Marsden, E. McCracken, S. DeWard, A. Barone, K. Hsu, E. Kakkis, Long-term major clinical outcomes in patients with long chain fatty acid oxidation disorders before and after transition to triheptanoin treatment—a retrospective chart review, *Mol. Genet. Metab.* 116 (1–2) (2015) 53–60.
- [28] A.E. Reszko, T. Kasumov, B.A. Pierce, F. David, C.L. Hoppel, W.C. Stanley, C. Des Rosiers, H. Brunengraber, Assessing the reversibility of the anaplerotic reactions of the propionyl-CoA pathway in heart and liver, *J. Biol. Chem.* 278 (37) (2003) 34959–34965.
- [29] X. Liu, Y. Qiao, X. Ting, W. Si, Isocitrate dehydrogenase 3A, a rate-limiting enzyme of the TCA cycle, promotes hepatocellular carcinoma migration and invasion through regulation of MTA1, a core component of the NuRD complex, *Am. J. Cancer Res.* 10 (10) (2020) 3212–3229.
- [30] S. Tohyama, J. Fujita, T. Hishiki, T. Matsuura, F. Hattori, R. Ohno, H. Kanazawa, T. Seki, K. Nakajima, Y. Kishino, M. Okada, A. Hirano, T. Kuroda, S. Yasuda, Y. Sato, S. Yuasa, M. Sano, M. Suematsu, K. Fukuda, Glutamine oxidation is indispensable for survival of human pluripotent stem cells, *Cell Metab.* 23 (4) (2016) 663–674.
- [31] C. Yang, B. Ko, Christopher T. Hensley, L. Jiang, Ajla T. Wasti, J. Kim, J. Sudderth, Maria A. Calvaruso, L. Lumata, M. Mitsche, J. Rutter, Matthew E. Merritt, Ralph J. DeBerardinis, Glutamine oxidation maintains the TCA cycle and cell survival during impaired mitochondrial pyruvate transport, *Mol. Cell* 56 (3) (2014) 414–424.
- [32] B. Ratnikov, P. Aza-Blanc, Z.E.A. Ronai, J.W. Smith, A.L. Osterman, D.A. Scott, Glutamate and asparagine cataplerosis underlie glutamine addiction in melanoma, *Oncotarget* 6 (10) (2015) 7379–7389.
- [33] B. Kim, J. Li, C. Jang, Z. Arany, Glutamine fuels proliferation but not migration of endothelial cells, *EMBO J.* 36 (16) (2017) 2321–2333.
- [34] R.I. Freshney, *Culture of Animal Cells*, 6. ed., Wiley-Blackwell, 2010.
- [35] A.J. Duncan, L.P. Hargreaves, M.S. Damian, J.M. Land, S.J. Heales, Decreased ubiquinone availability and impaired mitochondrial cytochrome oxidase activity associated with statin treatment, *Toxicol. Mech. Methods* 19 (1) (2009) 44–50.
- [36] A.J.M. Janssen, F.J.M. Trijbels, R.C.A. Sengers, J.A.M. Smeitink, L.P. van den Heuvel, L.T.M. Wintjes, B.J.M. Stoltenberg-Hogenkamp, R.J.T. Rodenburg, Spectrophotometric assay for complex I of the respiratory chain in tissue samples and cultured fibroblasts, *Clin. Chem.* 53 (4) (2007) 729.
- [37] P. Shelley, J. Tarry-Adkins, M. Martin-Gronert, L. Poston, S. Heales, J. Clark, S. Ozanne, J. McConnell, Rapid neonatal weight gain in rats results in a renal ubiquinone (CoQ) deficiency associated with premature death, *Mech. Ageing Dev.* 128 (11) (2007) 681–687.
- [38] L. Canevari, S. Kuroda, T.E. Bates, J.B. Clark, B.K. Siesjö, Activity of mitochondrial respiratory chain enzymes after transient focal ischemia in the rat, *J. Cereb. Blood Flow Metab.* 17 (11) (1997) 1166–1169.
- [39] O.H. Lowry, N.J. Rosebrough, A.L. Farr, R.J. Randall, Protein measurement with the folin phenol reagent, *J. Biol. Chem.* 193 (1) (1951) 265–275.
- [40] M.E. Skindersoe, M. Rohde, S. Kjaerulff, A novel and rapid apoptosis assay based on thiol redox status, *Cytometry A* 81 (5) (2012) 430–436.
- [41] M.E. Skindersoe, S. Kjaerulff, Comparison of three thiol probes for determination of apoptosis-related changes in cellular redox status, *Cytometry A* 85 (2) (2014) 179–187.
- [42] T. Welbourne, R. Routh, M. Yudkoff, I. Nissim, The glutamine/glutamate couplet and cellular function, *Physiology* 16 (4) (2001) 157–160.
- [43] A. Kuehne, H. Emmert, J. Soehle, M. Winnefeld, F. Fischer, H. Wenck, S. Gallinat, L. Terstegen, R. Lucius, J. Hildebrand, N. Zamboni, Acute activation of oxidative pentose phosphate pathway as first-line response to oxidative stress in human skin cells, *Mol. Cell* 59 (3) (2015) 359–371.
- [44] W. Wang, J. Palmfeldt, A.-W. Mohsen, N. Gregersen, J. Vockley, Fasting induces prominent proteomic changes in liver in very long chain acyl-CoA dehydrogenase deficient mice, *Biochem. Biophys. Res. Rep.* 8 (2016) 333–339.
- [45] S. Tucci, S. Primassin, U. Spiekerkoetter, Fasting-induced oxidative stress in very long chain acyl-CoA dehydrogenase-deficient mice, *FEBS J.* 277 (22) (2010) 4699–4708.
- [46] S. Tucci, D. Herebian, M. Sturm, A. Seibt, U. Spiekerkoetter, Tissue-specific strategies of the very-long chain acyl-CoA dehydrogenase-deficient (VLCAD^{-/-}) mouse to compensate a defective fatty acid β -oxidation, *PLoS one* 7 (9) (2012) e45429-e45429.
- [47] S. Tucci, U. Flögel, S. Hermann, M. Sturm, M. Schäfers, U. Spiekerkoetter, Development and pathomechanisms of cardiomyopathy in very long-chain acyl-CoA dehydrogenase deficient (VLCAD^{-/-}) mice, *Biochim. Biophys. Acta (BBA) - Mol. Basis Dis.* 1842 (5) (2014) 677–685.
- [48] H. Li, S. Fukuda, Y. Hasegawa, H. Kobayashi, J. Purevsuren, Y. Mushimoto, S. Yamaguchi, Effect of heat stress and bezafibrate on mitochondrial β -oxidation: comparison between cultured cells from normal and mitochondrial fatty acid oxidation disorder children using in vitro probe acylcarnitine profiling assay, *Brain Dev.* 32 (5) (2010) 362–370.
- [49] H. Li, S. Fukuda, Y. Hasegawa, J. Purevsuren, H. Kobayashi, Y. Mushimoto, S. Yamaguchi, Heat stress deteriorates mitochondrial β -oxidation of long-chain fatty acids in cultured fibroblasts with fatty acid β -oxidation disorders, *J. Chromatogr. B* 878 (20) (2010) 1669–1672.
- [50] Y. Wang, F.S. Yen, X.G. Zhu, R.C. Timson, R. Weber, C. Xing, Y. Liu, B. Allwein, H. Luo, H.-W. Yeh, S. Heissel, G. Unlu, E.R. Gamazon, M.G. Kharas, R. Hite, K. Birsoy, SLC25A39 is necessary for mitochondrial glutathione import in mammalian cells, *Nature* 599 (7883) (2021) 136–140.
- [51] V. Ribas, C. García-Ruiz, J.C. Fernández-Checa, Glutathione and mitochondria, *Front. Pharmacol.* 5 (2014).
- [52] S. Orloff, J.D. Butler, D. Towne, A.B. Mukherjee, J.D. Schulman, Pantetheinase activity and cysteamine content in cystinotic and normal fibroblasts and leukocytes, *Pediatr. Res.* 15 (7) (1981) 1063–1067.
- [53] P.L. Wood, M.A. Khan, J.R. Moskal, Cellular thiol pools are responsible for sequestration of cytotoxic reactive aldehydes: central role of free cysteine and cysteamine, *Brain Res.* 1158 (2007) 158–163.
- [54] R. Requejo, T.R. Hurd, N.J. Costa, M.P. Murphy, Cysteine residues exposed on protein surfaces are the dominant intramitochondrial thiol and may protect against oxidative damage, *FEBS J.* 277 (6) (2010) 1465–1480.
- [55] G. Gaston, J.A. Gangoiti, S. Winn, B. Chan, B.A. Barshop, C.O. Harding, M. B. Gillingham, Cardiac tissue citric acid intermediates in exercised very long-chain acyl-CoA dehydrogenase-deficient mice fed triheptanoin or medium-chain triglyceride, *J. Inherit. Metab. Dis.* 43 (6) (2020) 1232–1242.
- [56] M.B. Gillingham, S.B. Heitner, J. Martin, S. Rose, A. Goldstein, A.H. El-Gharbawy, S. Deward, M.R. Lasarev, J. Pollaro, J.P. DeLany, L.J. Burchill, B. Goodpaster, J. Shoemaker, D. Matern, C.O. Harding, J. Vockley, Triheptanoin versus trioctanoin for long-chain fatty acid oxidation disorders: a double blinded, randomized controlled trial, *J. Inherit. Metab. Dis.* 40 (6) (2017) 831–843.
- [57] E. Sklirow, A.N. Alodaib, S.F. Dobrowski, A.-W.A. Mohsen, J. Vockley, Physiological perspectives on the use of triheptanoin as anaplerotic therapy for long chain fatty acid oxidation disorders, *Front. Genet.* 11 (1651) (2021).
- [58] K. van Eunen, S.M. Simons, A. Gerding, A. Bleeker, G. den Besten, C.M. Touw, S. M. Houten, B.K. Groen, K. Krab, D.J. Reijngoud, B.M. Bakker, Biochemical competition makes fatty-acid beta-oxidation vulnerable to substrate overload, *PLoS Comput. Biol.* 9 (8) (2013), e1003186.
- [59] A.-C.M.F. Martinez, K. van Eunen, D.-J. Reijngoud, B.M. Bakker, The promiscuous enzyme medium-chain 3-keto-acyl-CoA thiolase triggers a vicious cycle in fatty-acid beta-oxidation, *PLoS Comput. Biol.* 13 (4) (2017), e1005461.
- [60] T. Sara, B. Sidney, S. Ute, De novo fatty acid biosynthesis and elongation in very long-chain acyl-CoA dehydrogenase-deficient mice supplemented with odd or even medium-chain fatty acids, *FEBS J.* 282 (21) (2015) 4242–4253.
- [61] S. Tucci, U. Floegel, F. Beermann, S. Behringer, U. Spiekerkoetter, Triheptanoin: long-term effects in the very long-chain acyl-CoA dehydrogenase-deficient mouse, *J. Lipid Res.* 58 (1) (2017) 196–207.
- [62] L. Gu, G.-F. Zhang, R.S. Kombu, F. Allen, G. Kutz, W.-U. Brewer, C.R. Roe, H. Brunengraber, Parenteral and enteral metabolism of anaplerotic triheptanoin in normal rats. II. Effects on lipolysis, glucose production, and liver acyl-CoA profile, *Am. J. Physiol. Endocrinol. Metab.* 298 (2) (2010). E362-E371.
- [63] V.P. Reddy, M.R. Garrett, G. Perry, M.A. Smith, Carnosine: a versatile antioxidant and antiglycating agent, *Sci. Aging Knowl. Environ.* 2005 (18) (2005) pe12.
- [64] A.A. Boldyrev, G. Aldini, W. Derave, Physiology and pathophysiology of carnosine, *Physiol. Rev.* 93 (4) (2013) 1803–1845.
- [65] A. Karaa, R. Haas, A. Goldstein, J. Vockley, W.D. Weaver, B.H. Cohen, Randomized dose-escalation trial of elamipretide in adults with primary mitochondrial myopathy, *Neurology* 90 (14) (2018) e1212–e1221, <https://doi.org/10.1212/WNL.0000000000005255>.